

Hydrogen-Bonding Interactions between Formic Acid and Pyridine

M. J. Fernandez-Berridi,[†] J. J. Iruin,[†] L. Irusta,[†] Jose M. Mercero,[‡] and Jesus M. Ugalde^{*‡}

Departamento de Ciencia y Tecnología de Polímeros, Facultad de Química, Universidad del País Vasco, Apdo. 1072, 20080 San Sebastián, Spain and Kimika Fakultatea, Euskal Herriko Unibertsitatea, P.K. 1072, 20080 Donostia, Euskadi, Spain

Received: November 9, 2001; In Final Form: January 18, 2002

The structure, energetics, vibrations, and barrier to internal rotation around the N \cdots H–O hydrogen bond of the binary pyridine–formic acid complex are calculated using one properly selected hybrid density functional theory procedure. The calculations demonstrate that the most stable isomer of the complex has a strong N \cdots H–O hydrogen-bonding interaction, whose strength is enhanced by the presence of an agostic interaction between the carbonylic oxygen and the α hydrogen of the pyridine. Rotation around N \cdots H–O, which prevents such an agostic interaction to occur, results in a decrease of the bonding energy of the complex from 11.1 kcal/mol to 6.43 kcal/mol. Additionally, a normal-mode analysis of the vibrations of the two most stable complexes characterized has been carried out and compared with the experimental vibrational frequencies of the pyridine–acetic acid complex. Furthermore, the effect of the specific solvation by one more formic acid molecule and one methanol molecule has also been considered. Both solvents enhance substantially the strength of the N \cdots H–O hydrogen bond as shown by the decrease of the N–H distance and the appreciable red shift of the O–H vibrational mode upon solvation.

I. Introduction

Hydrogen bonding¹ constitutes one salient structural element of clusters² and of many large molecules such as proteins, nucleic acids,³ and polymers.⁴ It is well known that hydrogen bonds might occur both within the same molecule (intramolecular) and between two different molecules (intermolecular). In either case, hydrogen bonding determines largely the geometrical structure of the resulting entity.

There are many examples in the literature that illustrate this point. Thus, recently, it has been reported that intramolecular hydrogen bonding, along with extensive intermolecular aromatic stacking, is the driving force which stabilizes double-stranded helices that are formed through dimerization of several carefully selected oligomers.⁵ This is in sharp contrast with the structure of other dimers formed by large molecules, including DNA,⁶ where hydrogen bonding determines the mode of interstrand association, and aromatic stacking takes place within each of the two different strands.

Equally relevant is the role played by hydrogen bonding in the sticking forces arising in the formation processes of interpolymer complexes. In particular, the nature of the interpolymer interaction between poly(carboxylic acid)s and poly(*n*-vinylpyridine) ($n = 2, 4$) has been a matter of great controversy. These carboxylic acid–pyridine systems may adopt two different proton-limiting structures, namely, OH \cdots N \rightleftharpoons O \cdots H⁺N, which yield hydrogen-bonding and ionic interpolymer interactions, respectively.

Probing the structure of these complexes has turned out to be rather challenging. However, substantial progress in the field has been led by Coleman and Painter,⁷ who have taken advantage of the fine sensitivity of FTIR spectroscopy to

hydrogen-bond interactions. In particular, analysis of the stretching bands of the carbonyl group allows the discrimination between those C=O groups which are engaged in hydrogen bonds and those which are not.⁸ The band corresponding to the ionic structure is found at smaller wavenumbers. Nevertheless, substantial care has to be exercised since the barrier of the proton between the two limiting structures is normally low;⁹ therefore, the experimental elucidation of the structure is difficult. Parallel progress has also been led by Lee et al.,¹⁰ who showed that X-ray photoelectron spectroscopy (XPS) might also be useful to unveil both ionic and hydrogen-bonding interactions in complexes involving poly(*n*-vinylpyridine) ($n = 2, 4$).

The interpolymer complexes formed by poly(acrylic acid) (PAA) and poly(methacrylic acid) (PMAA) with poly(2-vinylpyridine) (P2VPy) and poly(4-vinylpyridine) (P4VPy) have been the subject of considerable experimental effort. Thus, Fujimori et al.¹¹ and Inai et al.¹² reported the presence of hydrogen bonding between PAA or PMAA with P4VPy and PAA with P4VPy, respectively. On the other hand, Oyama and Nakajima¹³ found evidence of ionized carboxylic groups in PAA/P4VPy by infrared spectroscopy but were unable to find the signature of pyridinium ions in their XPS experiments. Finally, Zhou et al.,¹⁴ in a combined XPS and FTIR experimental investigation, showed that the interactions of PAA with both P4VPy and P2VPy were ionic, while their data for the corresponding PMAA complexes was very supportive of hydrogen-bonding type of interaction.

The plethora of experimental findings, mentioned above, indicate that the basis of the interaction between carboxylic acids and pyridine is not well understood. Therefore, fundamental studies are required to shed light on this interesting problem. With this in mind, we will study in this paper the hydrogen-bonded complexes of formic acid and pyridine. We will focus our main attention on the structural determination of the resulting clusters, because they serve as model systems for larger

* To whom correspondence should be addressed.

[†] Universidad del País Vasco.

[‡] Euskal Herriko Unibertsitatea.

aggregates. In addition, we will determine the nature and strength of the intermolecular bonding and finally, the experimentally relevant vibrations will be analyzed.

II. Computational Methods

All calculations were carried out with the GAUSSIAN98¹⁵ package. It has already been proven that the density functional theory (DFT) methods give excellent results in most chemical systems.¹⁶ The DFT hybrid methods correct the pure DFT overestimation of the bond dissociation energies,¹⁷ as validated by Johnson et al.¹⁸ The Becke proposed hybrid¹⁹(B3) together with the LYP²⁰ correlation functionals have been chosen for this work. Particularly relevant for the present investigation is the paper of Rablen et al.,²¹ who examined systematically the energies and structures of 53 hydrogen-bonded complexes of water with several various organic molecules. They concluded that B3LYP provides an affordable and reliable means of determining the strengths of hydrogen-bonding interactions, yielding dissociation energies in agreement with the best calculations available. Hence, for the sake of conciseness, we will not check further the appropriateness of B3LYP and will concentrate on the structure and vibrational spectra of the title complexes.

The all electron 6-311G split valence basis set augmented with a diffuse sp-set of functions and a polarization set of p- and d-functions has been used in this work (6-311++G(d,p)).

Frequencies were calculated at this level of theory and the corresponding zero-point vibrational energy (ZPVE) corrections were made to the total energy. All the calculated frequencies have been scaled down by 0.9613 as recommended by Wong.²² The binding energy was evaluated with the ZPVE corrected energies as $D_e = (E_A + E_B) - E_{AB}$, where AB stands for the complex, and A and B for each of the two molecules of the cluster. Since the basis set used in the present calculations is large enough, it is expected to yield a small basis set superposition error for the calculated dissociation energies. Indeed, for the least favorable case (structure **1**) the BSSE, estimated using the counterpoise method,^{23,24} is only 0.87 kcal/mol. Since this value is smaller than the accuracy of the computational method used to calculate it, we shall not consider hereafter corrections due to BSSE.

The Natural Bond Orbital²⁵ analysis was used to understand better the nature of the corresponding intermolecular interactions. Natural Bond Orbital analysis was performed on the polyatomic wave function²⁶ using the NBO program²⁷ of the GAUSSIAN package and the natural charges of the atoms were also evaluated. This method localizes the molecular orbitals and provides data that are in good agreement with the concepts of Lewis structures and the basic Pauling–Slater–Coulson picture of bond hybridization and polarization. For a good review of NBO and its applications, see the review article by Reed, Curtis, and Weinhold.²⁵

The MOLDEN²⁸ program was used to visualize and draw the figures.

III. Results and Discussion

A. Geometries. Several stable structures were found at the potential energy surface of the formic acid pyridine cluster. The most stable structures are shown in Figure 1.

Structure **1** is the most stable structure characterized in this study. Inspection of its geometry reveals the presence of two hydrogen-bonding interactions, namely, N···H–O and C–H···O. The relative orientation of the carboxylic acid is dictated by the linearity of the N···H–O hydrogen bond.

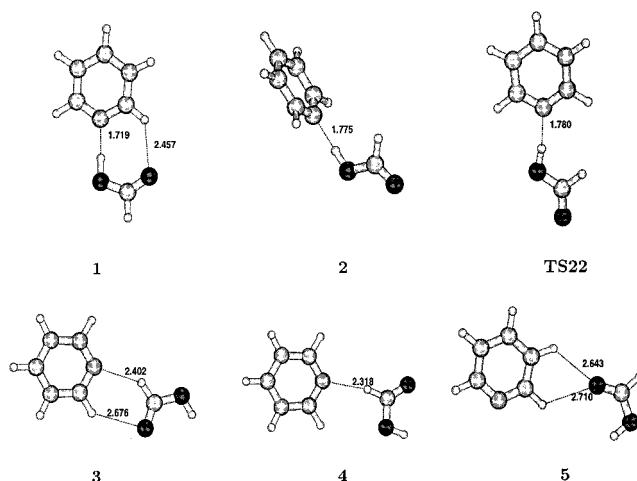


Figure 1. Geometries of the pyridine–formic acid binary complexes optimized at the B3LYP/6-311++G(d,p) level of theory. Distances shown are in angstroms.

The second most stable cluster is shown in Figure 1 as structure **2**. In this cluster the pyridine and the formic acid moieties lie in planes perpendicular to each other. Notice that the N···H distance has lengthened from 1.72 Å in **1** to 1.77 Å in **2**. This is a clear indication of a cooperative effect between the two hydrogen-bonding interactions of structure **1**. The presence of C–H···O hydrogen-bonding interaction in structure **1** strengthens the interaction between the pyridinic nitrogen and the acid hydrogen of the formic acid. We shall give more evidence of this effect in subsection IIIB. Notice that the relative orientation of the –COOH group around pyridine is now dictated by the linearity of the N···H–O hydrogen bond and the avoiding of the Fermi repulsion resulting from the α -agostic 4-electron interaction between the ortho hydrogen of the pyridine and the remaining hydrogen of the formic acid. Indeed, the planar structure resulting from rotating $\pi/2$ rad around the O–H single bond of the carboxylic acid, for which the Fermi repulsion is maximum, is the transition state that connects the two equivalent structures of **2** with respect to the molecular symmetry plane. Nevertheless, this Fermi repulsion is small and consequently, the N–H distance of the N···H–O hydrogen bond of **TS22**, 1.78 Å, is very similar to that of **2**, 1.77 Å.

Structure **3** is the next most stable isomer found. Inspection of its geometrical features indicates that there might be two hydrogen-bonding interactions, which are highlighted in Figure 1 as dotted lines. Notice, however, that none of them is linear. Also remarkable is the long distances between the hydrogens and their corresponding acceptor atoms. For the stronger hydrogen bond of **3**, that is, N···H–C, the N···H distance is 2.40 Å, 0.68 Å larger than its corresponding distance in structure **1**. The weakest hydrogen bond of **3** has a H···O distance of 2.68 which is 0.22 Å larger than its corresponding distance in **1**.

Structure **4**, shown in Figure 1, has one hydrogen-bonding interaction N···H–C, depicted in Figure 1 by a dotted line. The pseudolinearity of this bond precludes the relative orientation of the carboxylic acid with respect to the pyridine moiety in the cluster. The N···H length, 2.32 Å, of this hydrogen bond is slightly shorter than that of structure **3**, 2.40 Å. The distance between the α -hydrogen of the pyridine and the hydroxylic oxygen of the acid, 3.34 Å, is too large as to support a hydrogen-bonding interaction.

Finally, we have been able to characterize structure **5**. This cluster is held together by a tiny hydrogen-bonding interaction

TABLE 1: Binding Energies D_e (kcal/mol), the Donor ϕ_i and Acceptor ϕ_j Molecular Orbitals, and Their Corresponding Second-Order Interaction Energies $\Delta E_{ij}^{(2)}$ (kcal/mol) of the Hydrogen-Bonded Structures Shown in Figure 1

structure	D_e	$\phi_i \rightarrow \phi_j$	$E_{ij}^{(2)}$
1	11.10	$n_N \rightarrow \sigma_{O-H}^*$	34.24
		$n_O \rightarrow \sigma_{C-H}^*$	1.21
2	6.43	$n_N \rightarrow \sigma_{O-H}^*$	25.05
TS22	6.16	$n_N \rightarrow \sigma_{O-H}^*$	22.04
3	2.89	$n_N \rightarrow \sigma_{C-H}^*$	2.35
		$n_O \rightarrow \sigma_{C-H}^*$	0.79
4	2.60	$n_N \rightarrow \sigma_{C-H}^*$	5.07
		$n_O \rightarrow \sigma_{C-H}^*$	1.00
5	1.79	$n_N \rightarrow \sigma_{C-H}^*$	1.00
		$n_O \rightarrow \sigma_{C-H}^*$	1.00

between the carboxylic oxygen and the β -hydrogen of the pyridine. The C–H \cdots O distance is 2.64 Å. Inspection of Figure 1 reveals that the C–H \cdots O bond angle is far from linearity. Our optimized value is 124.6°.

Additionally, we have found two more stable structures involving hydrogen-bonding donor interactions with the ortho and meta and meta and para hydrogens of pyridine, respectively. However, these structures are predicted to be more unstable than the separated formic acid and pyridine fragments. They lie 2.23 and 2.19 kcal/mol higher in energy than the separated fragments, respectively. They should be seen as metastable structures with an expected small kinetic barrier toward fragmentation, since the potential energy surface is flat in this region. These structures are very unlikely to be detected.

B. Energetics. Table 1 collects the binding energies of the clusters characterized in this work. **1** has a binding energy of 11.1 kcal/mol. Remko²⁹ predicted a binding energy of 12.01 kcal/mol for the hydrogen-bonded system cluster of the acetic acid and pyridine. His semiempirical PCIO calculation agrees well with our value for the corresponding cluster of the formic acid.

The second most stable cluster, structure **2** has 4.67 kcal/mol less binding energy. Recall that **1** has two hydrogen-bonding interactions, N \cdots H–O and C–H \cdots O, while only the former is present in **2**. This might be tempting of ascribing a bonding energy of 6.43 kcal/mol to the N \cdots H–O hydrogen bond of **1** and 4.67 kcal/mol to the C–H \cdots O hydrogen bond of **1**. However, analysis of the NBO second-order interaction energies corresponding to these hydrogen-bonding interactions points to a different interpretation. The NBO second-order interaction energies are calculated as

$$\Delta E_{ij}^{(2)} = 2 \frac{|\langle \phi_i | \hat{F} | \phi_j \rangle|^2}{\epsilon_i - \epsilon_j} \quad (1)$$

where ϕ_i is the donor molecular orbital, ϕ_j is the acceptor molecular orbital, and ϵ_i and ϵ_j are their corresponding energy eigenvalues. $\Delta E_{ij}^{(2)}$ measures the strength of the donor–acceptor interaction between orbitals ϕ_i and ϕ_j and appears to be well suited to examine hydrogen-bonding interactions.³⁰

Inspection of Table 1 reveals that the N \cdots H–O hydrogen bond of structure **1** is remarkably strong, with a large second-order interaction energy of 34.24 kcal/mol. However, the C–H \cdots O hydrogen bond has a second-order interaction energy 1 order of magnitude smaller, that is, 1.21 kcal/mol. Therefore, the bulk of the bonding interaction in **1** should be ascribed to the N \cdots H–O hydrogen bond, being the contribution of the C–H \cdots O hydrogen-bonding interaction considerably smaller. Concomitantly, the N \cdots H–O hydrogen bond of **2** has a second-order interaction energy of 25.05 kcal/mol, which is substantially

TABLE 2: Frequency Shifts^a and Frequencies of Selected Hydrogen-Bond Vibrational Modes^b

structure	$\Delta\nu_1$	$\Delta\nu_2$	ν_{hbl}	ν_{hbs}	ν_3	ν_4
present work Py \cdots HCOOH						
1	14.8	776	120	192	78	1699
2	13.2	526	107	162		1758
6	16.8	875	110		79	1701
7	16.8	957	96		82	1634
experimental values for Py \cdots CH ₃ COOH						
	13.5	714–857	124	172	75	1700

^a Upon complexation of the fully symmetrical stretching vibration of pyridine, $\Delta\nu_1$, and of the stretching mode of the formic acid's H–O bond, $\Delta\nu_2$, in cm^{-1} . ^b Frequencies of the hydrogen-bond vibrational modes, ν_{hbl} , with more librational character and, ν_{hbs} , with more stretching character, in cm^{-1} . Frequencies of the stretching modes of CH \cdots O hydrogen bond, ν_3 , and of the C=O of the formic acid, ν_4 , in cm^{-1} .

smaller than the corresponding interaction energy of structure **1**. Namely, the weak C–H \cdots O hydrogen bond of **1** promotes an electronic rearrangement in the cluster resulting in a substantially stronger N \cdots H–O hydrogen-bonding interaction. This analysis suggests that despite its weakness, the C–H \cdots O hydrogen bond has a great influence on the overall binding energy of **1**.

As indicated in section IIIA, the planar structure of **2**, depicted in Figure 1 as **TS22**, corresponds to the transition state which connects the two equivalent structures of **2**, resulting from the inversion with respect to the pyridine plane. The energy barrier between these two equivalent minima is only 0.27 kcal/mol. This suggests that the rotation around the N \cdots H–O hydrogen bond of **2** is essentially free at room temperature. As expected, the second-order interaction energy of the N \cdots H–O hydrogen bond of **TS22** is very similar to that of **2**, see Table 1.

The weakly bound clusters **3**, **4**, and **5**, with binding energies of less than 3 kcal/mol, as shown in Table 1, have accordingly small second-order interaction energies.

C. Vibrational Spectra. The vibrational spectrum of the charge-transfer complex between pyridine and formic acid has not been reported so far. However, considerable effort has been paid to interpretation and assignment of the vibrational spectrum of the pyridine and acetic acid complex. We have collected in Table 2 the available experimental information on the complex between pyridine and acetic acid, along with our predictions for the pyridine–formic acid complex.

Mashkovsky and Odinkov³¹ found that the fully symmetrical stretching vibration of pyridine shifted 13.5 cm^{-1} toward higher frequencies upon complexation with the acetic acid. Our calculations, for the formic acid–pyridine complex, show that the A₁ fully symmetrical stretching vibration of pyridine has a frequency of 971.2 cm^{-1} , while the corresponding vibration for the most stable isomer of the complex, structure **1**, which has A' symmetry, has a frequency of 986.0 cm^{-1} , and the corresponding frequency for **2** is at 984.4 cm^{-1} . The shifts of this vibrational mode upon complex formation are, therefore, 14.8 cm^{-1} for **1** and 13.2 cm^{-1} for **2**, which agree well with the experimentally observed shift of the related acetic acid complex and puts forward the slight influence of the methyl group of the acidic moiety of the complex on this normal vibrational mode associated with the pyridine moiety.

In a related study, Langner and Zundel,⁹ reported the far-IR hydrogen-bond vibrations of the acetic acid–pyridine complex. They found two hydrogen-bond vibration bands at 124 and 172 cm^{-1} , respectively. The former has librational character with the carboxylic acid and the pyridine moieties performing a

pseudorotational motion against each other. The latter band has more stretching character. We have been able to characterize the normal modes associated with these two bands for our formic acid–pyridine complex. For structure **1**, they are predicted at 120.1 cm^{-1} and 192.3 cm^{-1} , respectively. These numbers agree well with both the experimental observation of the related acetic acid complex and the DFT/TZVP calculations of Langner and Zundel⁹ of 122 and 192 cm^{-1} , respectively, for the two hydrogen-bond vibrations of the latter complex. The corresponding frequencies of structure **2** have been calculated at 107.0 and 162.0 cm^{-1} , respectively.

Recently, Drichko et al.³² have measured the frequency of the hydrogen-bond vibration with stretching character in various solvents. Their data confirm the results of Langner and Zundel and in addition found that this band shifts toward higher frequencies in the series hexane, carbon tetrachloride, chloroform solvents. Such a frequency shift indicates that the strength of the $\text{N}\cdots\text{H}-\text{O}$ hydrogen bond interaction increases with the polarity of the solvent.³³

Nevertheless, for structure **1**, we have characterized another interesting vibrational mode at 77.6 cm^{-1} , which can be associated with the hydrogen-bond vibration with stretching character of the $\text{C}-\text{H}\cdots\text{O}$ hydrogen-bonding interaction of **1**. This band, which has a small predicted IR intensity of 4 km/mol , can also be appreciated as a small peak in the far-IR spectrum of monochloroacetic acid–pyridine complex as reported by Langner and Zundel in their figure 7 of reference 9. This is very supportive of the existence of such a weak hydrogen-bonding interaction between the α hydrogen of the pyridine with carboxylic oxygen of the formic acid, as we have put forward in section IIIB.

The absorption frequency of the stretching vibrational mode of the $\text{C}=\text{O}$ double bond of the carboxyl has been studied in detail by both Langner and Zundel⁹ and Drichko et al.³² Thus, Langner and Zundel found that the $\text{C}=\text{O}$ stretching band absorbs at 1720 cm^{-1} for the acetic acid–pyridine complex in chloroform at $20\text{ }^\circ\text{C}$. This band shifts to 1700 cm^{-1} on cooling to $-40\text{ }^\circ\text{C}$. Our calculations predict that the $\text{C}=\text{O}$ stretching vibrational mode of structure **1** of the formic acid–pyridine complex absorbs at 1699 cm^{-1} , in surprisingly nice agreement with the experimental observation. For structure **2**, the corresponding $\text{C}=\text{O}$ absorption frequency is calculated at 1758 cm^{-1} .

Drichko et al.,³² on the other hand, reported a band at 1725 cm^{-1} associated with the $\text{C}=\text{O}$ stretching vibrational mode for the complex formed between acetic acid and pyridine in hexane at room temperature and a Fermi resonance with the first overtone of the $\text{C}-\text{C}$ vibration of the acetic acid at 1755 cm^{-1} . Since, formic acid cannot have such a $\text{C}-\text{C}$ vibration, it is predicted that the Fermi resonance at 1755 cm^{-1} will be absent in the vibrational spectrum of the formic acid–pyridine complex.

The stretching mode of the $\text{O}-\text{H}$ of the carboxyl group involved in the $\text{N}\cdots\text{H}-\text{O}$ hydrogen bond undergoes a remarkable shift toward lower frequencies upon complexation. Thus, we have been able to identify such a vibrational mode for **1** at 2815 cm^{-1} , while the corresponding frequency of the formic acid has been found at 3591 cm^{-1} . The $\Delta\nu$ is 776 cm^{-1} for **1**. This should be compared with the $\Delta\nu$ of the $\text{C}=\text{O}$ stretching mode of only 45 cm^{-1} for the same structure. The frequency of the corresponding $\text{O}-\text{H}$ stretching of structure **2** is 3065 cm^{-1} , 250 cm^{-1} higher than **1**. This comes along with the weaker $\text{N}\cdots\text{H}-\text{O}$ hydrogen-bonding interaction of **2** relative to **1**, as discussed in section IIIB. Nevertheless, our calculations for structure **2** predict an absorption frequency at 2815 cm^{-1} ,

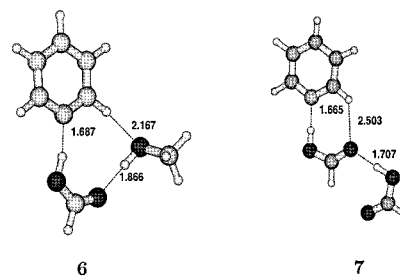


Figure 2. Geometries of the pyridine–formic acid–methanol, **6**, and pyridine–formic acid–formic acid, **7**, ternary complexes optimized at the B3LYP/6-311++G(d,p) level of theory. Distances shown are in angstroms.

although its intensity of 73.6 km/mol is 2 orders of magnitude smaller than that of the $\text{O}-\text{H}$ stretching. Further analysis of this mode reveals that it corresponds to the aliphatic $\text{H}-\text{C}$ stretching of the formic acid rather than to the $\text{O}-\text{H}$ stretching of the $\text{N}\cdots\text{H}-\text{O}$ hydrogen bond, as in **1**.

Experimental studies of the $\text{O}-\text{H}$ vibrational band of the carboxyl indicate that it has a strong dependence on the polarity of the solvent as reported by Drichko et al.³² They also found that the transition from the gas phase to solution decreases the absorption frequency of this band by $\sim 300\text{ cm}^{-1}$. Since their measured $\nu_{\text{O}-\text{H}}$ absorption frequencies lie within 2434 and 2577 cm^{-1} for solvents with different polarity, our calculated $\nu_{\text{O}-\text{H}}$ frequencies of 2815 and 3065 cm^{-1} for **1** and **2**, respectively, agree with their experimental results.

D. The Effect of Specific Solvation. We have considered the effect of the specific solvation of the formic acid fragment of the complex on the hydrogen-bonding interaction of our most stable cluster structure **1**. Methanol and one extra formic acid were chosen as “specific” solvent molecules. The former is normally used as the solvent in the preparation of the interpolymer complexes between polyacids and polypyridines.^{7,8,10–14} One optimized stable structure of each of these three fragment complexes are shown in Figure 2. We will like to emphasize that this paper is not aimed at a complete conformational investigation of the isomers of either **6** or **7**. Therefore, structures **6** and **7** of Figure 2 do not necessarily correspond with the *absolute* minimum energy structures of their corresponding potential energy surfaces. However, both structures are stable minima and therefore could be used to illustrate the effect of specific solvation.

Nevertheless, it is clear from the inspection of bond lengths given in Figure 2 that specific solvation of the carbonyl oxygen of the formic acid by either methanol or another formic acid molecule decreases substantially the $\text{N}\cdots\text{O}-\text{H}$ distance of the $\text{N}\cdots\text{O}-\text{H}$ hydrogen bond. Thus, for the methanol solvated complex the $\text{N}\cdots\text{H}$ distance shrinks 0.03 \AA , while for the formic acid solvated complex the corresponding reduction of the $\text{N}\cdots\text{H}$ distance is 0.05 \AA .

Concomitantly, we have observed, from the Natural Bonding Analysis of the electronic density, an increase of the strength of the $\text{N}\cdots\text{O}-\text{H}$ hydrogen-bonding interaction. Namely, for **6**, the second-order interaction energy between the nitrogen’s lone pair and the $\text{C}-\text{H}$ antibonding sigma orbital is 36.94 kcal/mol and for **7** is 42.25 kcal/mol . This higher strength of the intramolecular interactions in **7** is also reflected in its higher bonding energy: 20.0 kcal/mol , as compared to the 12.42 kcal/mol bonding energy of **6**.

The modifications of the vibrational spectrum of the complex induced by the solvent molecule are worth mentioning. Thus, while the symmetrical vibrational stretching of pyridine is hardly

affected by the presence of the solvent molecule, its frequency blue shifts 2 cm^{-1} for both **6** and **7**, relative to the unsolvated complex, the far-IR hydrogen-bond vibrations show large shifts. For instance, the vibrational mode with more librational character for **6** appears at 110 cm^{-1} and at 96 cm^{-1} for **7**. Both frequencies are red shifted 8 cm^{-1} and 24 cm^{-1} , respectively, with respect to the unsolvated structure **1**. The mode with more stretching character is slightly blue shifted, by 2 and 5 cm^{-1} for **6** and **7**, respectively. These results are in accordance with a stronger $\text{N}\cdots\text{H}-\text{O}$ hydrogen-bonding interaction in the "solvated" complexes.

The $\text{C}=\text{O}$ stretching of the methanol solvated complex **6** is also slightly blue shifted with respect to **1**. Our calculations predict a tiny shift of only 2 cm^{-1} . However, for the formic acid solvated complex the $\text{C}=\text{O}$ stretching is predicted at 1634 cm^{-1} , namely, 65 cm^{-1} lower than the unsolvated complex **1**. Remarkably, we have found that the $\text{C}=\text{O}$ stretching of the solvating formic acid absorbs at 1701 cm^{-1} . This is a well known fact that associated—the ones involved in hydrogen bonds— $\text{C}=\text{O}$ acid groups resonate at lower frequencies.^{8,32}

Finally, the $\text{O}-\text{H}$ stretching of the carboxyl group involved in the $\text{N}\cdots\text{H}-\text{O}$ hydrogen bond is appreciably red shifted upon specific complexation by either methanol or formic acid. The corresponding $\nu_{\text{O}-\text{H}}$ absorption frequency of **6** is calculated at 2716 cm^{-1} , 99 cm^{-1} lower with respect to **1**. The corresponding shift for **7** is predicted to be a remarkable 181 cm^{-1} , with its $\text{O}-\text{H}$ vibrating at 2634 cm^{-1} . These highlight nicely the reduction of the $\text{O}-\text{H}$ bond strength in the series **1**, **6**, **7**, which can hardly be anticipated by the inspection of their corresponding bond length increase, 1.007 \AA for **1**, 1.018 \AA for **6**, and 1.022 \AA for **7**.

IV. Conclusions

Pyridine and formic acid orient preferably parallel to each other on the same molecular plane. This maximizes the hydrogen-bonding interaction between the N and the $\text{H}-\text{O}$ of the formic acid. By the same token, this orientation allows for a second weak hydrogen-bonding interaction between the $\alpha\text{ C}-\text{H}$ of the pyridine and the carboxylic oxygen of the formic acid. Nevertheless, it triggers a remarkable cooperative effect as revealed by the much larger bonding energy of the planar structure **1** with respect to the nonplanar perpendicularly oriented structure **2**, where the $\alpha\text{ C}-\text{H}\cdots\text{O}$ hydrogen-bonding interaction is absent.

Recall that the bonding energy of the perpendicularly oriented isomer, structure **2**, is only 6.16 kcal/mol , as compared with the bonding energy of 11.10 of the in-plane arranged isomer, structure **1**.

Stable isomers with aliphatic hydrogens engaged in the hydrogen-bonding interaction either with the nitrogen of the pyridine or with the $\text{C}=\text{O}$ of the acid lie much higher in energy, as expected from the reduced acidity of aliphatic hydrogens. Thus, structures **3**, **4**, and **5** are very weakly bound, by less than 3 kcal/mol , with respect to their fragments, which hampers their experimental detection.

The normal analyses of the structures **1** and **2** agree nicely with the reported experimental mid- and far-IR frequencies of the related pyridine-acetic acid complex. Additionally, our calculations suggest that the tiny peak observed at the low end of the far-IR region could be assigned to the librational mode of the agostic hydrogen-bonding interaction of structure **1**. This feature has passed without remark up to date.

Finally, as shown in the discussion of structures **6** and **7**, we have found that specific solvation of the most stable complex isomer **1** leads to a strengthening of the $\text{N}\cdots\text{H}-\text{O}$ hydrogen

bond. This is best seen by inspection of the corresponding $\text{O}-\text{H}$ vibrational frequencies. Our calculation predicts a red shift for the $\text{O}-\text{H}$ vibration of 99 cm^{-1} for the methanol solvated structure **6** and 181 cm^{-1} for the formic acid solvated structure **7**, with respect to the unsolvated structure **1**.

Acknowledgment. This research was funded by Euskal Herriko Unibertsitatea (the University of the Basque Country), Gipuzkoako Foru Aldundia (the Provincial Government of Guipuzkoa), Eusko Jaurlaritz (the Basque Government), and Ministerio de Ciencia y Tecnología (Spanish Office of Science and Technology).

References and Notes

- (1) Scheiner, S. *Hydrogen Bonding. A Theoretical Perspective*; Oxford University Press: New York, 1997.
- (2) Ugalde, J. M.; Alkorta, I.; Elguero, J. *Angew. Chem., Int. Ed. Engl.* **2000**, *39*, 717.
- (3) Baker, E. N.; Hubbard, R. E. *Prog. Biophys. Mol. Biol.* **1984**, *44*, 97.
- (4) Jiang, M.; Qun, X.; Qin, W.; Fei, L. *Macromolecules* **1995**, *28*, 710.
- (5) Berl, V.; Huc, I.; Khoury, R. G.; Krische, M. J.; Lehn, J. M. *Nature* **2000**, *407*, 720.
- (6) Stryer, L. *Biochemistry*; W. H. Freeman and Company: New York, 1988.
- (7) Coleman, M. M.; Painter, P. C. *Appl. Spectrosc. Rev.* **1984**, *20*, 255.
- (8) Fernandez-Berridi, M. J.; Iruin, J. J.; Iriando, P. *Macromolecules* **1996**, *29*, 5605.
- (9) Langner, R.; Zundel, G. *J. Chem. Soc., Faraday Trans.* **1995**, *91*, 3831.
- (10) Goh, S. H.; Lee, S. Y.; Dai, J.; Tan, K. L. *Polymer* **1996**, *37*, 5305.
- (11) Fujimori, K.; Trainor, G. T.; Costigan, M. J. *J. Polym. Sci., Polym. Chem. Ed.* **1984**, *22*, 2479.
- (12) Inai, Y.; Kato, S.; Hirabayashi, T.; Yokota, K. *J. Polym. Sci., Part A: Polym. Chem.* **1996**, *34*, 2341.
- (13) Oyama, H.; Nakajima, T. *J. Polym. Sci., Polym. Chem. Ed.* **1983**, *21*, 2897.
- (14) Zhuo, X.; Goh, S. H.; Lee, S. Y.; Tan, K. L. *Polymer* **1998**, *39*, 3631.
- (15) Frisch, M. J.; Trucks, G. W.; Schlegel, H. B.; Scuseria, G. E.; Robb, M. A.; Cheeseman, J. R.; Zakrzewski, V. G.; Montgomery, J. A.; Stratmann, R. E.; Burant, J. C.; Dapprich, S.; Millam, J. M.; Daniels, A. D.; Kudin, K. N.; Strain, M. C.; Farkas, O.; Tomasi, J.; Barone, V.; Cossi, M.; Cammi, R.; Mennucci, B.; Pomelli, C.; Adamo, C.; Clifford, S.; Ochterski, J.; Petersson, G. A.; Ayala, P. Y.; Cui, Q.; Morokuma, K.; Malick, D. K.; Rabuck, A. D.; Raghavachari, K.; Foresman, J. B.; Cioslowski, J.; Ortiz, J. V.; Stefanov, B. B.; Liu, G.; Liashenko, A.; Piskorz, P.; Komaromi, I.; Gomperts, R.; Martin, R. L.; Fox, D. J.; Keith, T.; Al-Laham, M. A.; Peng, C. Y.; Nanayakkara, A.; Gonzalez, C.; Challacombe, M.; Gill, P. M. W.; Johnson, B. G.; Chen, W.; Wong, M. W.; Andres, J. L.; Head-Gordon, M.; Replogle, E. S.; Pople, J. A. *Gaussian 98*, a5; Gaussian, Inc.: Pittsburgh, PA, 1998.
- (16) Labanowsky, J.; Andelzelm, J. *Density Functional Methods in Chemistry*; Springer-Verlag: New York, 1991.
- (17) Tschinke, V.; Ziegler, T. *Theor. Chim. Acta* **1991**, *81*, 651.
- (18) Johnson, B. G.; Gill, P. M. W.; Pople, J. A. *J. Chem. Phys.* **1993**, *98*, 5612.
- (19) Becke, A. D. *J. Chem. Phys.* **1993**, *98*, 5648.
- (20) Lee, C.; Yang, W.; Parr, R. G. *Phys. Rev. B* **1998**, *37*, 785.
- (21) Rablen, P. R.; Lockman, J. W.; Jorgensen, W. L. *J. Phys. Chem. A* **1998**, *102*, 3782.
- (22) Wong, M. W. *Chem. Phys. Lett.* **1996**, *256*, 391.
- (23) Boys, S. F.; Bernardi, F. *Mol. Phys.* **1970**, *19*, 553.
- (24) Schwenke, D. W.; Truhlar, D. W. *J. Chem. Phys.* **1985**, *82*, 2418.
- (25) Reed, A. E.; Curtiss, L. A.; Weinhold, F. *Chem. Rev.* **1988**, *88*, 899.
- (26) Foster, J. P.; Curtiss, L. A.; Weinhold, F. *J. Am. Chem. Soc.* **1980**, *88*, 899.
- (27) Glendening, E. D.; Reed, A. E.; Carpenter, J. E.; Weinhold, F. Nbo version 3.1.
- (28) Molden; see <http://www.cmbi.kun.nl/~schafv/molden/molden.html>.
- (29) Remko, M. *Adv. Mol. Relax. Interaction Process.* **1980**, *16*, 155.
- (30) Glendening, E. D.; Badenhop, J. K.; Weinhold, F. *J. Comput. Chem.* **1998**, *19*, 628.
- (31) Mashkovsky, A. A.; Odinkov, S. E. *Spectrosc. Lett.* **1974**, *7*, 271.
- (32) Drichko, N. V.; Kerenskaia, G. Y.; Schreiber, V. M. *J. Mol. Struct.* **1999**, *477*, 127.
- (33) Schreiber, V. M.; Shchepkin, D. N. *J. Mol. Struct.* **1992**, *270*, 351.